**TRANSVERSE AND TORSIONAL SHEAR STRESSES
IN PRISMATIC BODIES HAVING INHOMOGENEOUS MATERIAL
PROPERTIES
USING A NEW 2D STRESS FUNCTION**

Lampros C. Kourtis, Haneesh Kesari, Dennis R. Carter
and Gary S. Beaupré

# TRANSVERSE AND TORSIONAL SHEAR STRESSES
# IN PRISMATIC BODIES HAVING INHOMOGENEOUS MATERIAL PROPERTIES
# USING A NEW 2D STRESS FUNCTION

LAMPROS C. KOURTIS, HANEESH KESARI, DENNIS R. CARTER AND GARY S. BEAUPRÉ

We introduce a new formulation to concurrently calculate torsional and transverse shear stresses in prismatic beams with homogeneous or inhomogeneous material properties. This new formulation is generated using kinematic assumptions for the torsion problem and using a new stress function for the transverse shear problem that accounts for Poisson effects. The effect of gradients in material properties is captured explicitly as body forces. The results using this new formulation are compared to full three-dimensional solutions and show good agreement ($l^2$ error metric in the order of $10^{-4}$), while both modeling and computational costs are significantly lower. The numerical implementation of this new formulation can be used to analyze stresses in arbitrary cross sections ranging from structural members (civil) to long bones (biomechanics) with either homogeneous or inhomogeneous material properties.

## 1. Introduction

The problem of out-of-plane shear stress calculation in cross sections of prismatic beams presents significant interest in a variety of applications ranging from structural engineering to biomechanics. Out-of-plane shear stresses are created by either torsional or transverse loads. In most cases, the two problems of torsional shear and transverse shear have been addressed separately.

In cases of simple cross sectional geometries, elementary mechanics of materials approaches to the transverse shear problem [Young and Budynas 2002; Goodier 1962] yield approximations of the stress distribution and of the maximum stress values. Depending on the application however, these approximations might underestimate the actual stresses present: for example, for a square cross section, the maximum shear stress value may be underestimated by up to 18% (for $\nu = 0.5$) while for a circular cross section the maximum shear stress value may be underestimated by up to 12% (for $\nu = 0$) [Barber 1992]. For more detailed analysis, the exact two-dimensional elasticity solution that describes the complete out-of-plane shear stress distribution is developed and applied to analytically described cross sections (such as the ellipse or the rectangle) in many classical elasticity textbooks [Barber 1992; Timoshenko and Goodier 1984; Sokolnikoff 1956].

The torsional shear problem is addressed more frequently in the literature. Many textbooks [Timoshenko and Goodier 1984; Sokolnikoff 1956] present the generalized problem under the Saint-Venant assumption and solve it for specific analytically described cross sections (such as the ellipse, rectangle). Structural engineering elements (such as I-beams) under torsion may be studied by expanding the solution of the rectangle (primitive) to each of the discrete subregions of the cross section with special considerations at the junctions where primitives meet [Goodier 1962]. Thin-walled closed sections (such

as cellular shapes) are usually studied using Bredt's formulas by adding an analogue of Kirchhoff's law for shells [Gjelsvik 1981; Timoshenko and Goodier 1984; Schulz and Filippou 1998]. Sokolnikoff [1956] discusses the inhomogeneous beam problem, for a finite number of components having different elastic properties, where additional boundary conditions are imposed at their interfaces.

The finite element method has been used to address the problem of torsion of cross sections of arbitrary shape using a two-dimensional formulation. Herrmann [1965] presented a solution to the torsion problem of homogeneous beams based on the Saint-Venant assumption and a numerical formulation using the Ritz technique. A computer implementation using the Galerkin formulation, called VA-TWIST, to analyze homogeneous, prismatic beams subjected to torsional loading was developed by [Levenston et al. 1994]. Mason and Herrmann [1968] proposed a finite element formulation to the transverse shear problem by minimizing the total potential energy of an unknown warping function across the section. An alternative formulation [Gruttmann et al. 1999] introduces a warping function for torsion and two new functions for transverse shear — one for the pure transverse shear contribution and one for the effect of Poisson's ratio due to flexure, all solved numerically using the finite element method. Reissner [1979; 1983; 1993] used the principle of minimum complementary energy to derive seven differential equations of equilibrium to determine stresses in the complex problem of axial, bending, transverse and torsional loads. However, these formulations are sometimes difficult to implement in a numerical solution [Gruttmann et al. 1999]. They also regard bodies as homogeneous, failing thus to capture inhomogeneity contributions, an important factor in biomechanics [Kourtis et al. 2008] or composite materials studies. Muskhelishvili [1963] derived the governing equations to calculate torsional stresses in beams containing different reinforcing materials; the equations can lead to closed-form or series solutions for simple geometries.

The goal of this paper is to present a new method to determine shear stresses caused by torsional and transverse shear loads on an arbitrarily-shaped prismatic body having inhomogeneous material properties. This new formulation is obtained by superimposing two relatively simple solutions, one for torsion (derived from an assumed displacement field) and one for transverse shear (derived from an assumed strain field).

Routinely, elasticity problems are reformulated by introducing stress functions. For example, in the Airy stress function formulation in plane elasticity, stresses are constructed as derivatives of an unknown function in a manner such that the equilibrium conditions are automatically satisfied; the problem then only requires solving the compatibility equations subject to the boundary conditions. The stress function itself has no obvious physical interpretation in this case. The problem can also be reformulated such that compatibility is automatically satisfied; the problem then only requires solving the equilibrium equations subject to the boundary conditions. An example of this approach is the Love strain function in the axisymmetric elasticity problem [Barber 1992]. The elasticity formulation presented in this work follows this second approach.

## 2. Materials and methods

A prismatic body is subjected to far-field transverse and torsional loads (Figure 1); $\Omega$ represents the cross section interior, $\Gamma$ denotes the boundary of the section such that $\Omega \cap \Gamma = 0$. The $x$ and $y$ axes lie in-plane; the $z$ axis defines the out-of-plane direction. At the section under examination, there exist an angular twist $\theta$ (or alternatively torsion $T$ in cases where the center of shear coincides with the centroid) and
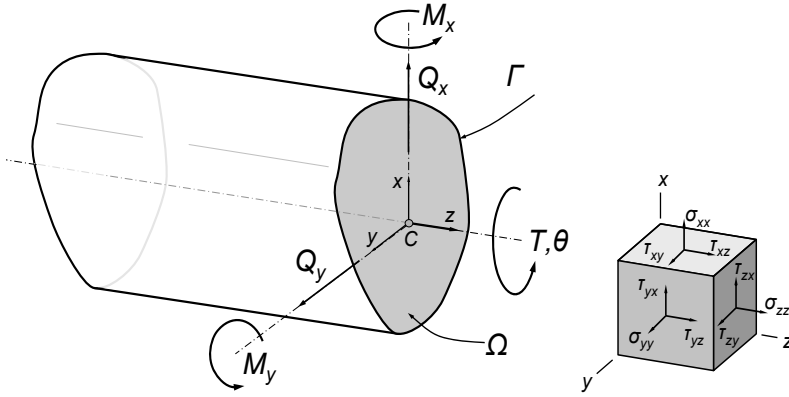
**Figure 1.** A prismatic beam with Cartesian coordinate system. Bending moments $M_x$, $M_y$ transverse shear forces $Q_x$, $Q_y$ and angular twist $\theta$ and torque $T$ are shown at a representative cross section. Transverse shear and torsional loads create shear stresses $\tau_{zx}$ and $\tau_{zy}$.

transverse forces $Q_x$ and $Q_y$ (obtained easily using the method of sections) as well as bending moments $M_x$ and $M_y$.

Since the cross section has inhomogeneous material properties, the effective centroid $C : (C_x^*, C_y^*)$ is defined in both integral and finite element form as in [Carpenter et al. 2005]:

$$(C_x^*, C_y^*) = \left( \frac{\int x E(x, y) dA}{\int E(x, y) \, dA}, \ \frac{\int y E(x, y) \, dA}{\int E(x, y) \, dA} \right) = \left( \frac{\sum x_i A_i E_i}{\sum A_i E_i}, \ \frac{\sum y_i A_i E_i}{\sum A_i E_i} \right), \tag{1}$$

where $i$ enumerates the elements, $x_i$, $y_i$ are the element's centroid coordinates, $A_i$ is its area and $E_i$ its elastic modulus.

For convenience, we shift the coordinate system so the effective centroid $(C_x^*, C_y^*)$ is at the origin:

$$(C_x^*, C_y^*) = (0, 0). \tag{2}$$

The flexural rigidities $I_{xx}^*$, $I_{yy}^*$ about the axes, the generalized moment of inertia $I_{xy}^*$ and the axial stiffness are calculated using inhomogeneous beam theory [Carpenter et al. 2005]:

$$I_{xx}^* = \int y^2 E(x, y) \, dA = \sum ((I_{xx}^e E)_i + y_i^2 A_i E_i), \tag{3}$$

$$I_{yy}^* = \int x^2 E(x, y) \, dA = \sum ((I_{yy}^e E)_i + x_i^2 A_i E_i), \tag{4}$$

$$I_{xy}^* = \int xy E(x, y) \, dA = \sum ((I_{xy}^e E)_i + x_i y_i A_i E_i), \tag{5}$$

$$A^* = \int E(x, y) \, dA = \sum A_i E_i, \tag{6}$$

where the sum runs over all elements and $I_{xx}^e$, $I_{yy}^e$, $I_{xy}^e$ denote each element's moment of inertias about its centroid.

Transverse forces $Q_x$, $Q_y$ applied to the body at a distance $z$ from the cross section under examination cause bending stresses. Ignoring any axial forces and assuming small strains, the normal stresses in the longitudinal direction $\sigma_{zz}$ are given as in [Bartel et al. 2006]:

$$\sigma_{zz} = \left( \frac{Q_x I_{xx}^* - Q_y I_{xy}^*}{I_{xx}^* I_{yy}^* - I_{xy}^{*\,2}} E_i x_i + \frac{Q_y I_{yy}^* - Q_x I_{xy}^*}{I_{xx}^* I_{yy}^* - I_{xy}^{*\,2}} E_i y_i \right) \cdot z. \tag{7}$$

The prismatic bar with the given cross section and properties under torsional and/or transverse loads is examined away from the points of load application to avoid stress concentrations. Although transverse shear and torsion can be solved separately and the stresses can then be superimposed, we developed a single formulation to address transverse shear and torsion simultaneously.

***Transverse shear.*** Euler-Bernoulli beam theory assumes that the out-of-plane normal stress varies linearly with the distance $z$, but the theory neglects Poisson effects. In this section we use classical elasticity to derive the transverse shear stress distribution due to bending in a prismatic beam of arbitrary cross section and inhomogeneous material properties. For this analysis, we make the following assumptions:

- $\sigma_{xx} = \sigma_{yy} = \tau_{xy} = 0$.

- $\tau_{zx}$, $\tau_{zy}$ are independent of $z$.

- The normal stress $\sigma_{zz}$ varies as described in (7).

- The Poisson's ratio $\nu$ is constant across $\Omega$.

- $G$, $E$ are arbitrary spatial functions of $x$, $y$, at least piecewise continuous across $\Omega$.

For notational convenience, we introduce

$$\alpha = \frac{Q_x I_{xx}^* - Q_y I_{xy}^*}{I_{xx}^* I_{yy}^* - I_{xy}^{*\,2}} \qquad \text{and} \qquad \beta = \frac{Q_y I_{yy}^* - Q_x I_{xy}^*}{I_{xx}^* I_{yy}^* - I_{xy}^{*\,2}}, \tag{8}$$

so (7) becomes

$$\sigma_{zz} = [\alpha \cdot x \cdot E(x, y) + \beta \cdot y \cdot E(x, y)] \cdot z. \tag{9}$$

The assumptions above on stress imply the following constraints on strain from linear elasticity:

$$\varepsilon_{xx} = -\frac{\nu}{E(x, y)} \sigma_{zz}, \quad \varepsilon_{yy} = -\frac{\nu}{E(x, y)} \sigma_{zz}, \quad \varepsilon_{zz} = -\frac{1}{E(x, y)} \sigma_{zz}, \quad \gamma_{xy} = 0. \tag{10}$$

The form of $\gamma_{zx}$ and $\gamma_{zy}$ is still unknown. However from the assumptions we know that $\gamma_{zx}$ and $\gamma_{zy}$ are not functions of $z$. Therefore:

$$\gamma_{zx} = \frac{\tau_{zx}}{G(x, y)} \qquad \text{and} \qquad \gamma_{zy} = \frac{\tau_{zy}}{G(x, y)}. \tag{11}$$

Further information about the form of $\gamma_{zx}$ and $\gamma_{zy}$ can be found using the compatibility conditions. We therefore assume the following form for $\gamma_{zx}$ and $\gamma_{zy}$ that satisfies compatibility:

$$\gamma_{zx} = \phi_{,x} - 2\beta\nu xy, \quad \gamma_{zy} = \phi_{,y} - 2\alpha\nu xy, \tag{12}$$

where a subscript variable after a comma indicates partial differentiation with respect to that variable. The unknown function $\phi = \phi(x, y)$ is $C^2$ continuous in $\Omega$.

It is easy to see that the six compatibility relations (13) are satisfied either identically (left column and first equality on second column), or due to the definition of shear strain in (12):

$$\varepsilon_{xx,yy} + \varepsilon_{yy,xx} = \gamma_{xy,xy}, \qquad 2\varepsilon_{zz,xy} = \gamma_{yz,xz} + \gamma_{xz,yz} - \gamma_{xy,zz},$$
$$\varepsilon_{yy,zz} + \varepsilon_{zz,yy} = \gamma_{yz,yz}, \qquad 2\varepsilon_{xx,yz} = -\gamma_{yz,xx} + \gamma_{xz,xy} + \gamma_{xy,xz}, \tag{13}$$
$$\varepsilon_{xx,zz} + \varepsilon_{zz,xx} = \gamma_{xz,xz}, \qquad 2\varepsilon_{yy,xz} = \gamma_{yz,xy} - \gamma_{xz,yy} + \gamma_{xy,yz}.$$

From (11) and (12) we obtain the following form for transverse shear stresses due to bending:

$$\tau_{zx} = G(x, y)(\phi_{,x} - 2\beta\nu xy), \qquad \tau_{zy} = G(x, y)(\phi_{,y} - 2a\nu xy). \tag{14}$$

Equation (14) will be used later in the development of the strong form of the problem. Having provided a form for the transverse shear using a stress function, we proceed to find a form for the torsional shear using kinematic assumptions. We then superimpose the two to satisfy equilibrium.

*Torsional shear.* In this section we derive the torsional shear stress distribution in a beam of arbitrary cross section and inhomogeneous material properties due to torsion based on kinematic relations (Saint-Venant) for a presumed displacement field and for small deformations.

For this analysis, the following assumptions are made:

- $\sigma_{xx} = \sigma_{yy} = \sigma_{zz} = \tau_{xy} = 0$.

- $\tau_{zx}$, $\tau_{zy}$ are independent of $z$.

- $G$ is an arbitrary spatial function of $x$, $y$, at least piecewise continuous across $\Omega$.

Using similar notation as in the previous section, the in-plane torsional displacements $u_x$, $u_y$ vary linearly with the distance from the centroid of the cross section $(C_x^*, C_y^*)$ and are given by:

$$u_x = -\theta \cdot y \cdot z, \qquad u_y = \theta \cdot x \cdot z, \tag{15}$$

where $\theta$ is the linear angle of twist.

Torsion is assumed to occur around the effective centroid of the cross section; the same relations hold for off-centroid torsion cases by replacing $(C_x^*, C_y^*)$ with the center of rotation $(C_x, C_y)$.

A function $\psi$, called the warping function, is chosen such that the out-of-plane displacements $u_z$ caused by torsion are given by

$$u_z = \theta \cdot \psi(x, y). \tag{16}$$

Since we assume a displacement field, the compatibility equations are automatically satisfied. From (16) we derive a relation for the torsional shear strains:

$$\gamma_{xz} = u_{z,x} + u_{x,z}, \qquad \gamma_{yz} = u_{z,y} + u_{y,z}. \tag{17}$$

Assuming linear isotropic or transverse isotropic elastic material properties, substituting (15) and (16) in (17), and employing the constitutive relations we obtain

$$\tau_{xz} = G(x, y)\theta(\psi_{,x} - y), \qquad \tau_{yz} = G(x, y)\theta(\psi_{,y} + x). \tag{18}$$

*Governing relations and boundary conditions.* The equations for equilibrium can be written in compact notation as $\sigma_{ij,j} = 0$. The two equilibrium relations in $x$ and $y$ directions are identically satisfied due to the nature of the assumptions. The third equilibrium equation yields

$$\sigma_{zz,z} + \tau_{zx,x} + \tau_{zy,y} = 0. \tag{19}$$

Invoking linear superposition we combine expressions (18) and (14), for the stresses arising respectively from torsion and transverse shear, with (19), obtaining

$$E(\alpha x + \beta y) + (G(\theta \psi_{,x} - \theta y + \phi_{,x} - 2\beta \nu x y))_{,x} + (G(\theta \psi_{,y} + \theta x + \phi_{,y} - 2\alpha \nu x y)) = 0, \tag{20}$$

where $G, E$ are given functions of $x, y$. It is useful to combine the two unknown functions $\psi, \phi$ by setting

$$\Xi \overset{\text{def}}{=} \theta \psi + \phi. \tag{21}$$

The scalar function $\psi$, due to the nature of the kinematic assumptions, can be interpreted as a measure of the out of plane deformations $(u_z)$, and is called the warping function; the scalar function $\varphi$, however, lends itself to no such physical interpretation.

Simplifying the preceding expression yields the governing equation for the combined transverse shear and torsional shear problem:

$$(G\Xi_{,x})_{,x} + (G\Xi_{,y})_{,y} = 2\nu x y(\beta G_{,x} + \alpha G_{,y}) - (E - 2G\nu)(\alpha x + \beta y) + \theta(G_{,x} y - G_{,y} x) = f(x, y). \tag{22}$$

Note that for an isotropic elastic solid, $E$ can be replaced by

$$E = 2(1 + \nu)G. \tag{23}$$

The boundary conditions are obtained by imposing zero traction at the boundaries $\Gamma$:

$$\tau_{zx} \cdot n_x + \tau_{zy} \cdot n_y = 0 \quad \text{on } \Gamma, \tag{24}$$

where $\boldsymbol{n}$ is the normal vector to the boundary $\Gamma$. Combining the stresses arising from the torsion (18) and the transverse shear (14) in (24), and recalling (21), we obtain

$$G(\Xi_{,i} n_i) = G\big((\theta y + 2\beta \nu x y)n_x - (\theta x - 2\alpha \nu x y)n_y\big) \quad \text{on } \Gamma. \tag{25}$$

Using (22) and (25), the strong form of the shear problem becomes:

*Given $\alpha, \beta, \theta$ and functions $G(x, y)$ and $E(x, y)$, find $\Xi \in C^2$ such that*

$$\begin{aligned} (G\Xi_{,i})_{,i} &= f(x, y) \ \ on \ \Omega, \\ G\Xi_{,i} n_i &= Gt_i n_i \quad on \ \Gamma, \end{aligned} \tag{26}$$

*where*

$$f(x, y) = 2\nu x y(\beta G_{,x} + \alpha G_{,y}) - (E - 2G\nu)(\alpha x + \beta y) + \theta(G_{,x} y - G_{,y} x), \quad t = \begin{bmatrix} \theta y + 2\beta \nu x y \\ -\theta x + 2\alpha \nu x y \end{bmatrix}. \tag{27}$$

The function $f(x, y)$ can be thought of as body force and $\boldsymbol{t}$ can be thought of as a traction vector. The importance of the material property gradient terms $G_{,x}$ and $G_{,y}$ in the expression of $f(x, y)$ will be discussed later.

***Finite element approximation.*** Based on the strong form definition of the problem just given, we introduce the trial function space

$$\Upsilon = \{w \mid w \in \mathcal{H}^1 \text{ on } \Omega\},$$

which provides the weak form as

$$\int_{\Omega} w \left( G \Xi_{,ii} + G_{,i} \Xi_{,i} - f(x, y) \right) d\Omega = 0 \quad \text{for all } (x, y) \in \Omega, \tag{28}$$

$$\int_{\Omega} w (G \Xi_{,i})_i d\Omega = \int_{\Omega} w f(x, y) d\Omega. \tag{29}$$

Integrating by parts and using the divergence theorem we get

$$\int_{\Gamma} (w G \Xi_{,i}) n_i d\Gamma - \int_{\Omega} w_{,i} G \Xi_i d\Omega = \int_{\Omega} w f(x, y) d\Omega. \tag{30}$$

After incorporating the boundary conditions we obtain the weak form of the problem:

*Given $\alpha, \beta, \theta$ and functions $G(x, y)$ and $E(x, y)$, find $\Xi \in \Upsilon$ such that*

$$\int_{\Omega} w_{,i} G \Xi_{,i} d\Omega = \int_{\Gamma} w G t_i n_i d\Gamma - \int_{\Omega} w f(x, y) d\Omega, \tag{31}$$

*where $f(x, y)$ and $\boldsymbol{t}$ are as in (27).*

Introducing the finite element function space and element shape functions [Hughes 2000] we have

$$k_{ab}^e = \int_{\Omega^e} N_{a,i}^e G^e N_{b,i}^e d\Omega^e, \tag{32}$$

where $a$ and $b$ range over the nodes and superscript $e$ refers to the element space; $G^e$ is the shear modulus assigned to the element. Moreover

$$f_a^e = (f_a^f)^e + (f_a^g)^e, \qquad \text{with} \quad (f_a^f)^e = -\int_{\Omega^e} N_a^e f(x, y) d\Omega^e, \quad (f_a^g)^e = \int_{\Gamma^e} N_a^e G t_i n_i d\Gamma^e.$$

Note that $(f_a^f)^e$ can be easily computed using Gauss quadrature. The gradients of the shear modulus can be calculated using the shape function derivatives:

$$G_{,x} = \int N_{a,x} G_a d\Omega, \qquad G_{,y} = \int N_{a,y} G_a d\Omega^e, \tag{33}$$

where $G_a$, the shear modulus for node $a$, can be taken as the average of the shear modulus values $G^e$ of the elements sharing that node.

The shear stresses are calculated from (14), (18) and (21) as

$$\tau_{zx} = G(x, y)(\Xi_{,x} - 2\beta v x y - \theta y), \qquad \tau_{zy} = G(x, y)(\Xi_{,y} - 2\alpha v x y + \theta x). \tag{34}$$

The torque, $T$, corresponding to the given angular twist $\theta$ can be calculated by integrating over the element stress contributions weighted linearly by their distance from the centroid:

$$T = \int_{\Omega} (x \tau_{zy} - y \tau_{zx}) d\Omega, \tag{35}$$

or by substituting the stresses from (34) and, since $\phi = 0$ (no transverse shear), by replacing $\Xi = \theta \psi$ from (21):

$$T = \int_\Omega G(x, y)(x \, \Xi_{,y} - y \, \Xi_{,x}) \, d\Omega. \tag{36}$$

The integral term in (35) and (36) is called the torsional rigidity and is denoted by $K^*$. Note that (36) provides the net torque $T$ supported by the prismatic beam when it is subjected to an angular twist about its effective centroid.

The numerical implementation of this formulation can be downloaded from https://simtk.org/home/ va-batts.

## 3. Results

*Validation examples.* In the case of torsionless bending of a homogeneous body having an idealized geometry (circle or rectangle), the new formulation in (26)–(27) reduces to the relations provided in [Timoshenko and Goodier 1984], and a numerical comparison has been provided [Kourtis et al. 2008]. Similarly, in the case of pure torsion of a homogeneous body having those geometries, the new formulation reduces to the relations provided in [Barber 1992]. In addition, we numerically compared the solution to several problems of torsionless bending of homogeneous bodies having arbitrary geometries provided in [Gruttmann et al. 1999] to the solutions obtained using the new formulation, obtaining excellent agreement (results not shown).

Several representative cross sectional geometries are presented and analyzed in this section. We provide a verification of the new formulation by comparison to the three-dimensional elasticity solution, for the homogeneous and inhomogeneous material property cases. Comparison of the 2D model using the new formulation to a 3D elasticity model is the only way to validate models having arbitrary cross sections and inhomogeneous material properties; in addition, the 3D model is generated by extruding the 2D mesh conveniently guaranteeing correspondence between node and integration point locations.

**Example 1** (Homogeneous elliptic beam). A solid elliptical beam subjected to transverse loads and to torsion was analyzed using the new formulation and the results compared to the three-dimensional solution. The axis lengths were taken as $a = 100$ mm and $b = 60$ mm, and the elastic modulus as 1 MPa. The cross section was meshed using 924 quadrilateral 4-node elements. The predicted shear stresses $\tau$ from the new formulation were compared to the three-dimensional solution, $\tau_{3D}$ (Figure 2). The three-dimensional solution was found using an extruded model, that was composed of 19,404 elements, analyzed with ABAQUS. The number of element layers in the out-of-plane (extruded) direction was chosen in order to maintain an element aspect ratio of less than 10 to 1. The $l^2$ error metric

$$l^2 = \sqrt{\frac{(\tau - \tau_{3D})^2}{\tau_{3D}^2}} \tag{37}$$

was found to be $3.25 \times 10^{-4}$.

**Example 2** (Homogeneous I-beam). A standard structural member, the steel I-beam, was subjected to torsional and transverse shear loads, in the form of an about-the-centroid torsional displacement (angle of twist) and a vertical transverse load. The dimensions of the cross section are given in Figure 3.
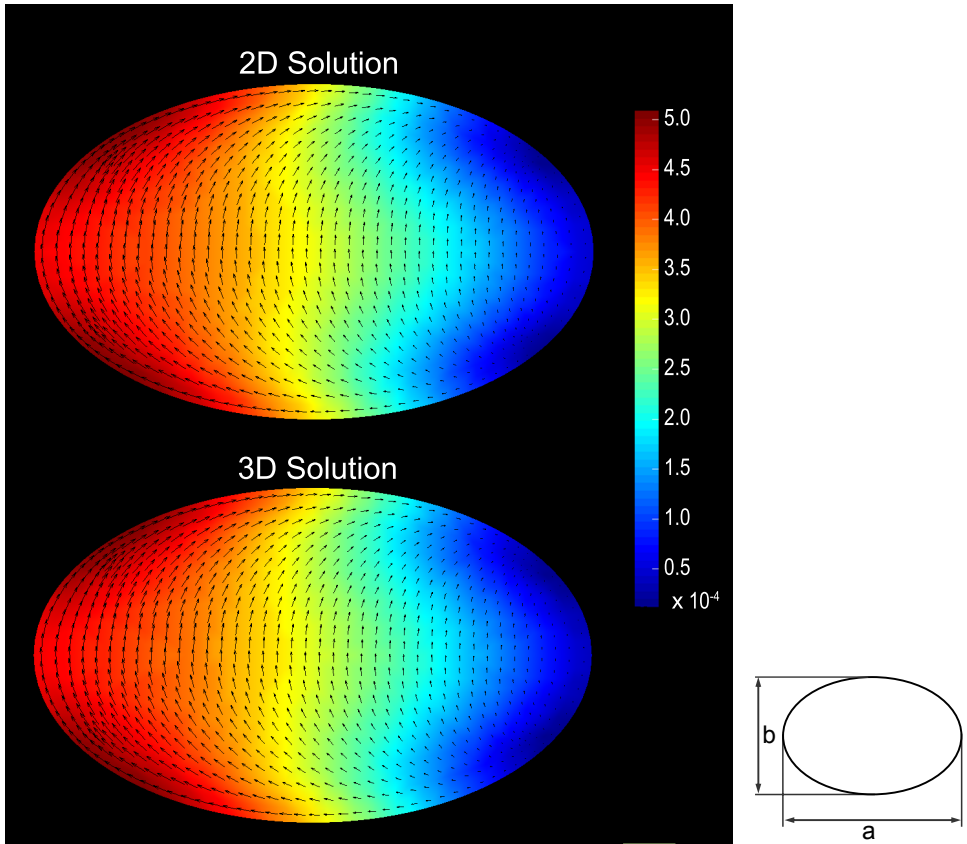
**Figure 2.** Validation example 1: A homogeneous beam with an elliptic cross section (axis lengths $a = 100$ mm and $b = 60$ mm), with an elastic modulus $E = 1$ MPa, is subjected to a transverse force of 1 N acting in the vertical direction and applied through the centroid, combined with an applied angular twist of $3.5 \times 10^{-7}$ degree/mm. The resulting shear stresses [MPa] demonstrate minimal stress on the right side and maximum stress on the left side; the transverse shear stresses are either decreased or increased by the torsional shear stresses. Top: solution obtained with the new two-dimensional implementation (1,954 DOF). Bottom: representative cross section of the solution obtained with a full, three-dimensional finite element analysis (61,551 DOF). The $l^2$ error metric is $3.25 \times 10^{-4}$.

Since analytical solutions for this cross section are only approximations of the elasticity solution, a full three-dimensional model was created and analyzed. The cross section was meshed using 946 linear quadrilateral 4-node elements and stresses were calculated using the proposed formulation. The same two-dimensional mesh was extruded, yielding 23 element layers to produce a three-dimensional prismatic beam composed of 21,758 linear 8-node hex elements, 2.5 times longer than the height of the I-beam. As in Example 1, the number of element layers in the out-of-plane direction was chosen in order to maintain an element aspect ratio of less than 10 to 1. The boundary conditions were applied to the prism by fully
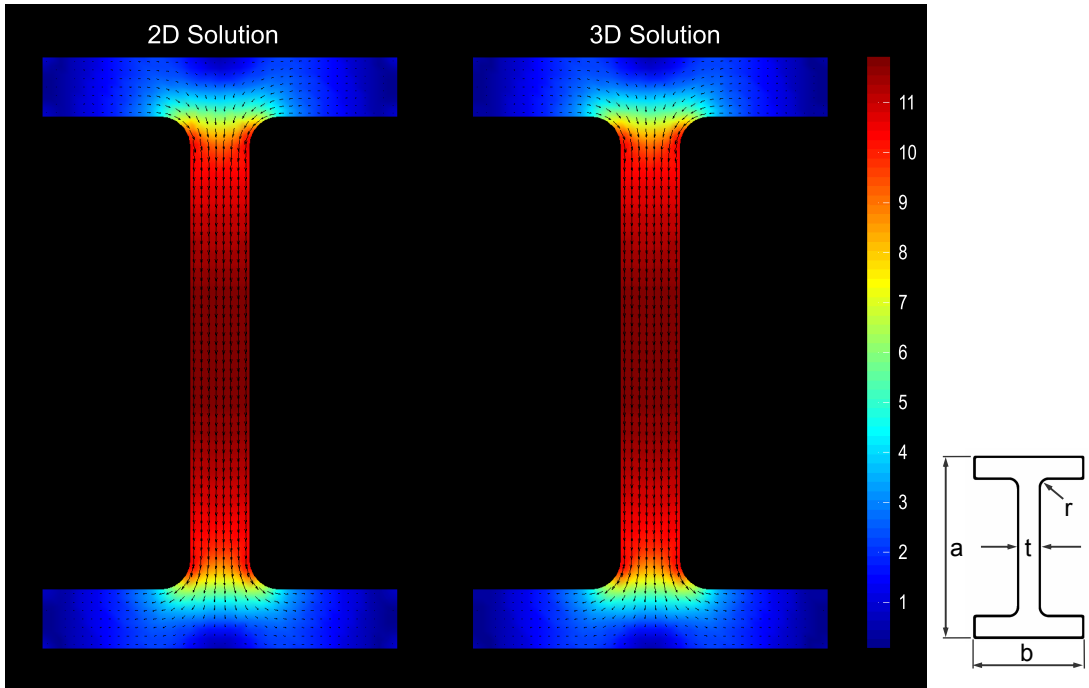
**Figure 3.** Validation example 2: A homogeneous I-beam ($a = 100$ mm, $b = 60$ mm, $t = 10$ mm, $r = 5$ mm) with elastic modulus 100 MPa is subjected to a transverse force of 100 N acting in the vertical direction and applied through the centroid. No torsion or twist is applied. The resulting shear stresses (MPa) are shown for the new two-dimensional implementation (left; 2,166 DOF) and for the full, three-dimensional finite element analysis (right; 74,727 DOF). $l^2$ error metric: $7.72 \times 10^{-4}$.

constraining the nodes of one end and by tying [ABAQUS 2002] the nodes of the other end to a reference point, which was then subjected to the transverse force and the angular twist. Stresses calculated using the two-dimensional model were compared to the three-dimensional solution (Figure 3). The location for comparison within the three-dimensional model was chosen so as not to be influenced by any stress concentrations associated with the imposed boundary conditions. In this case, the $l^2$ error metric was found to be $7.72 \times 10^{-4}$. One source of error using the proposed two-dimensional formulation is the poor definition of the normals at the corner elements, which causes artifacts.

**Example 3** (Inhomogeneous rectangle: steel reinforced concrete beam). A solid rectangular beam, subjected to a transverse force and to a torsional twist around its centroid, was analyzed using the new formulation. The results were then compared to the three-dimensional solution. The dimensions of the beam and the rebar elements and the magnitudes of the applied loads are given in Figure 4. Steel was modeled to be 7 times stiffer than concrete [Hendy and Johnson 2006]. No-slip conditions were assumed between the steel rebar and the concrete. The cross section was meshed using 2,507 linear quadrilateral 4-node elements. As in the I-beam example, the two-dimensional mesh was extruded to produce a three-dimensional prismatic beam composed of 67,689 linear 8-node hex elements and the boundary conditions
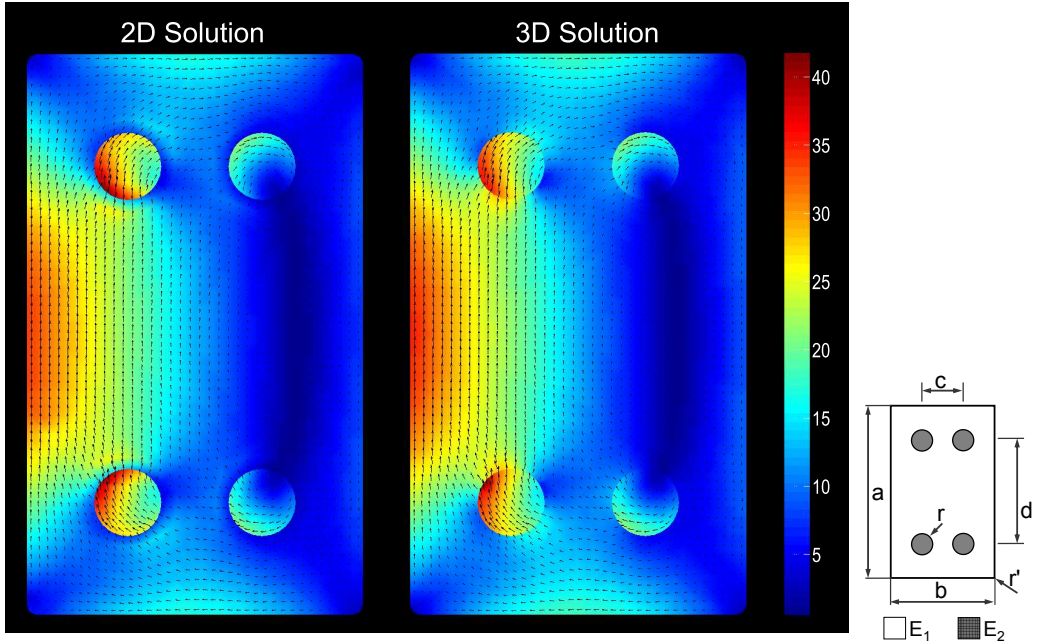
**Figure 4.** Validation example 3: A rectangular beam made of concrete containing rebar (the four circles), with dimensions $a = 100$ mm, $b = 60$ mm, $c = 30$ mm, $d = 50$ mm, $r = 6$ mm, $r' = 1$ mm, is subjected to 50 kN of transverse force applied in the vertical direction through the centroid along with $3.5 \times 10^{-7}$ degree/mm of angular twist about its centroid. The rebar material ($E_2 = 200{,}000$ MPa) is approximately seven times stiffer than the concrete material ($E_1 = 29{,}000$ MPa). The plot shows the shear stresses in the two materials, along with the shear stress direction. The resulting shear stresses [MPa] are shown both for the new two-dimensional implementation (left; 5,220 DOF) and for the full, three-dimensional finite element analysis (right; 211,410 DOF). $l^2$ error metric: $8.31 \times 10^{-3}$.

were applied respectively. The stress calculated using the proposed formulation is in good agreement with that derived from the three-dimensional model (Figure 4), with an $l^2$ error metric of $8.31 \times 10^{-3}$.

*Application example: Inhomogeneous cross section of a bone instrumented with a cemented prosthesis.* We next considered an example involving a complex biomechanical application: a hip replacement in which a metallic stem is inserted into the intramedullary canal of the femur and orthopaedic cement fills the remaining space. Bone is by nature a highly inhomogeneous material; its density and its elastic modulus vary from site to site. Using well established methods, tomographic X-ray images can provide information on the local bone density and hence the elastic modulus at each location within the cross section. After creating the finite element mesh to represent the bone cross section, each element was assigned an individual set of material properties corresponding to the local (element) image properties [Kourtis et al. 2008]. The longitudinal elastic modulus, $E(x, y)$, was found to range from 2,000 MPa to 17,500 MPa throughout the cross section. The shear modulus of the bone was then calculated according to
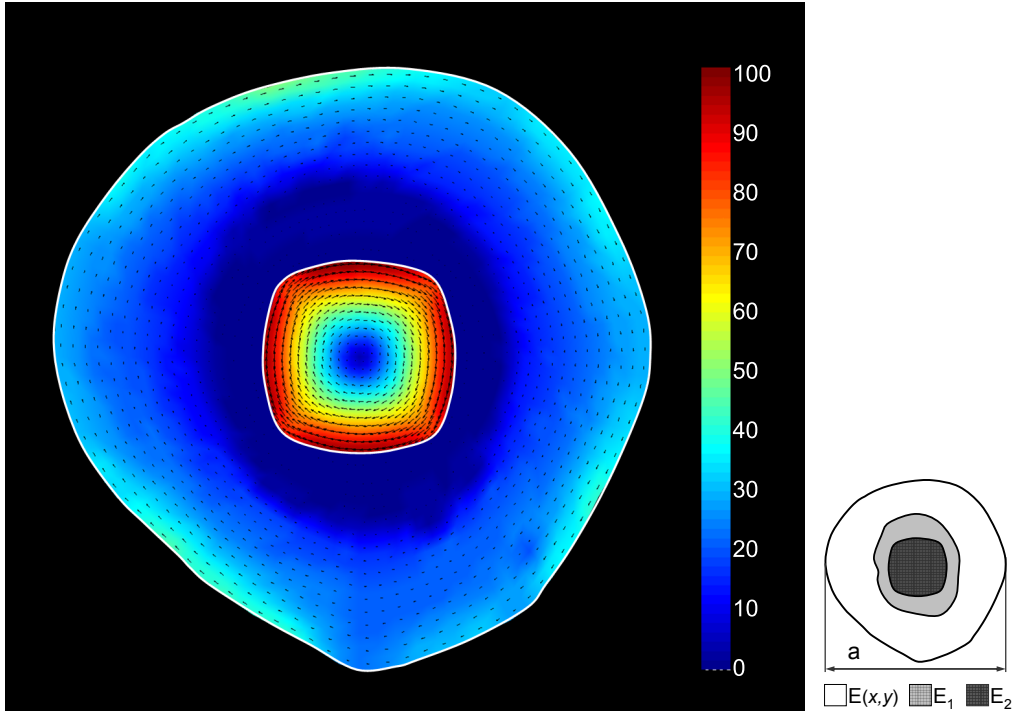
**Figure 5.** Stresses (MPa) are shown for a model consisting of the shaft of the femur ($a \sim 23$ mm) with a titanium alloy prosthesis cemented within the intramedullary cavity. The applied torsional and transverse shear loads were estimated for stair ascent. The maximum shear stress within the bone was 52.64 MPa whereas the maximum shear stress within the implant was 98.23 MPa. The highest PMMA cement shear stress close to the metal implant was 2.17 MPa.

the relation $G = 0.19E$ introduced in [Reilly and Burstein 1975]. An implant made of titanium Ti6Al4V alloy (elastic modulus $E_2 = 114,000$ MPa) was assumed to be inserted in the intramedullary canal, and orthopedic cement (PMMA) with elastic modulus $E_1 = 2,350$ MPa [Williams and Johnson 1989] fills the remaining space between the bone and the implant. The model was subjected to torsional and peak transverse loads ($F_{M-L} = 0.59$ BW, $F_{A-P} = 0.61$ BW, $T_z = 2.24$ BW m, where BW $= 80$ kg is the body weight), corresponding to a stair climbing load case obtained from biomechanical studies [Bergmann et al. 2001]. The problem was then solved using the new two-dimensional formulation (Figure 5). Since this is a closed section that is approximately axisymmetric, we made the assumption that the center of shear coincides with the effective centroid of the cross section [Tapley and Poston 1990]. The analysis showed that the maximum shear stress within the bone was 52.64 MPa, while the maximum shear stress within the implant was 98.23 MPa. Stresses in the PMMA cement were significantly lower, and went up to 2.17 MPa near the metal implant interface. Studies have shown that the metal-cement interface shear stress limit depends on the surface treatment (roughness) of the implant; for a grit-blasted metal surface the interface shear stress limit is reported in the order of 7.8–8.61 MPa [Müller and Schürmann 1999].

## 4. Discussion

The mathematical method presented in this article provides a straightforward means of accurately calculating torsional and transverse shear stresses of a prismatic beam having inhomogeneous material properties, and at low computational cost since no three-dimensional solution is needed. As seen from the results, comparison to the "gold standard" three-dimensional solutions, shows extremely low $l^2$ error metrics. Depending on the needs, the new formulation can be either used to calculate pure torsional shear, or pure transverse shear or combination thereof. The new formulation can also be used to analyze beams with either homogeneous or inhomogeneous material properties.

Amongst other features, this formulation provides a chance to explore "torqueless" twisting during which a beam will twist even though it is only subjected to transverse loads. This may occur because of the geometry and/or inhomogeneity of the beam as well as the direction and location of the applied transverse load. Torqueless twisting will occur if transverse forces are not applied through the center of shear. In addition, a beam only subjected to an angular twist about an axis other than the center of shear will undergo bending as if it were loaded by a transverse load. However, in closed solid sections, such as the ones examined in this study, the center of shear is very close to the effective centroid [Tapley and Poston 1990], therefore the assumption made in the torque calculation section that they coincide.

It is interesting to take a closer look at the terms in the strong form of the problem, Equations (26)–(27), and quantify their contribution to the overall result. The function $f(x, y)$ right-hand side of the domain equation has three terms: the first and last represent the effects of the gradients of material properties on the calculation of shear stresses created by the transverse load and the angular displacement, respectively. In the transverse shear case, this gradient term is "activated" as a result of a Poisson effect. The Poisson effect is also responsible for the second term in the boundary condition equation; without this, the transverse shear stress distribution would vary in one direction only. In order to quantify the importance of these terms we examined the case of an inhomogeneous square beam containing an insert that is one-third as stiff as the rest of the beam. We calculated stresses using (26)–(27) and then recalculated stresses after omitting the material property gradient terms (Figure 6). A qualitative inspection of the plots indicates that both the absolute values of the stress as well as the stress distribution are affected by the presence of these terms. More specifically, the highest stress for the torsion problem differed by $-7.7\%$ while for the transverse shear problem the difference was $-4.1\%$. These differences are expected to be even larger for larger mismatches between the various properties of the beam; for example, if the shear moduli of the two materials in this example had a tenfold difference, the maximum stresses would differ by $-10.5\%$ and $-5.9\%$ for the torsion and the transverse shear problems, respectively.

One of the limitations of the new formulation is that unlike the elastic and shear moduli $(E, G)$ that are spatial functions across the domain $\Omega$, Poisson's ratio remains constant. Still, using this formulation, one could vary Poisson's ratio for each element according to some spatial function and obtain approximate results; however (26) does not include terms that correspond to the spatial gradient of the Poisson's ratio. Another limitation of the formulation is that it can only be used with isotropic or transverse isotropic materials; anisotropic and orthotropic material models inherently cannot be described by this two-dimensional approach.

The new formulation offers an easier and faster method to determine shear stresses compared with a full, three-dimensional approach. In terms of computational cost, in order to maintain the same element
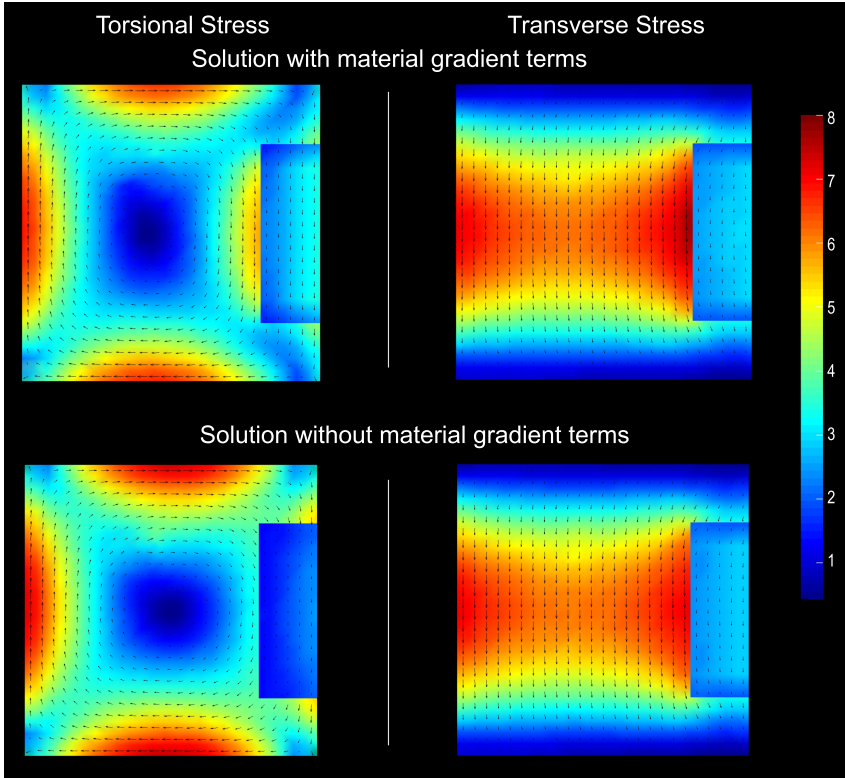
**Figure 6.** Importance of the material property gradient terms in Equations (26)–(27). A square beam with an insert (right), one-third as stiff. Left: torsional stresses [MPa]. The absolute stress values are different and the overall distribution changes with the incorporation of the material property gradient terms. Right: transverse stresses [MPa]. Here there is less difference between the solutions with and without the shear modulus spatial gradient terms, but the latter solution underestimates shear stresses.

aspect ratio, it can be shown that the number of three-dimensional elements must increase as the number of two-dimensional elements raised to the 1.5 power. In addition, the three-dimensional elements would have an extra degree of freedom for each node, again rendering the two-dimensional solution more attractive (see comparison of degrees of freedom for the 2D and 3D cases in captions of Figures 1–3). Especially in cases where multiple analysis are needed, such as in plasticity or fatigue studies, the computational cost benefit of the two-dimensional approach can be substantial. Second, a three-dimensional model requires an extrusion meshing step after the original two-dimensional mesh creation, which along with the material properties assignment can prove time consuming. Most commercial software meshing packages do not offer the option of "inheriting" material properties from a two-dimensional parent mesh to its three-dimensional extruded mesh. In addition, coupling the torsion and the transverse shear problems into one, further decreases the computational requirements. Also, the application of boundary conditions in a three-dimensional model is not always trivial, as for example at least one end may need to be constrained relative to a reference point to which the actual displacements or loads are applied.

## Acknowledgments

## References

[ABAQUS 2002] *ABAQUS theory manual*, Hibbitt, Karlsson and Sorensen, Inc., Providence, RI, 2002.

[Barber 1992] J. R. Barber, *Elasticity*, Kluwer, Dordrecht, 1992.

[Bartel et al. 2006] D. L. Bartel, D. T. Davy, and T. M. Keaveny, *Orthopaedic biomechanics: mechanics and design in musculoskeletal systems*, 1st ed., Pearson/Prentice Hall, Upper Saddle River, NJ, 2006.

[Bergmann et al. 2001] G. Bergmann, G. Deuretzbacher, M. Heller, F. Graichen, A. Rohlmann, J. Strauss, and G. N. Duda, "Hip contact forces and gait patterns from routine activities", *J. Biomech.* **34**:7 (2001), 859–871.

[Carpenter et al. 2005] R. D. Carpenter, G. S. Beaupré, T. F. Lang, E. S. Orwoll, and D. R. Carter, "New QCT analysis approach shows the importance of fall orientation on femoral neck strength", *J. Bone Miner. Res.* **20**:9 (2005), 1533–1542.

[Gjelsvik 1981] A. Gjelsvik, *The theory of thin walled bars*, Wiley, New York, 1981.

[Goodier 1962] J. N. Goodier, "Torsion", pp. 1–27 in *Handbook of engineering mechanics*, edited by W. Flugge, McGraw-Hill, New York, 1962.

[Gruttmann et al. 1999] F. Gruttmann, R. Sauer, and W. Wagner, "Shear stresses in prismatic beams with arbitrary cross-sections", *Int. J. Numer. Methods Eng.* **45**:7 (1999), 865–889.

[Hendy and Johnson 2006] C. R. Hendy and R. P. Johnson, *Designers' guide to EN 1994-2: Eurocode 4: design of composite steel and concrete structures*, Thomas Telford, London, 2006.

[Herrmann 1965] L. R. Herrmann, "Elastic torsional analysis of irregular shapes", *J. Eng. Mech.* (*ASCE*) **91**:6 (1965), 11–19.

[Hughes 2000] T. J. R. Hughes, *The finite element method: linear static and dynamic finite element analysis*, Dover, Mineola, NY, 2000. Pages 60–70.

[Kourtis et al. 2008] L. C. Kourtis, D. R. Carter, H. Kesari, and G. S. Beaupré, "A new software tool (VA-BATTS) to calculate bending, axial, torsional and transverse shear stresses within bone cross sections having inhomogeneous material properties", *Comput. Methods Biomech. Biomed. Engin.* **11**:5 (2008), 463–476.

[Levenston et al. 1994] M. E. Levenston, G. S. Beaupré, and M. C. van der Meulen, "Improved method for analysis of whole bone torsion tests", *J. Bone Miner. Res.* **9**:9 (1994), 1459–1465.

[Mason and Herrmann 1968] W. E. Mason and L. R. Herrmann, "Elastic shear analysis of general prismatic beams", *J. Eng. Mech.* (*ASCE*) **94**:4 (1968), 965–983.

[Müller and Schürmann 1999] R. T. Müller and N. Schürmann, "Shear strength of the cement metal interface: an experimental study", *Arch. Orthop. Trauma Surg.* **119**:3–4 (1999), 133–138.

[Muskhelishvili 1963] N. I. Muskhelishvili, *Some basic problems of the mathematical theory of elasticity: fundamental equations, plane theory of elasticity, torsion, and bending*, Noordhoff, Groningen, 1963.

[Reilly and Burstein 1975] D. T. Reilly and A. H. Burstein, "The elastic and ultimate properties of compact bone tissue", *J. Biomech.* **8**:6 (1975), 393–405.

[Reissner 1979] E. Reissner, "Some considerations on the problem of torsion and flexure of prismatical beams", *Int. J. Solids Struct.* **15**:1 (1979), 41–53.

[Reissner 1983] E. Reissner, "Further considerations on the problem of torsion and flexure of prismatical beams", *Int. J. Solids Struct.* **19**:5 (1983), 385–392.

[Reissner 1993] E. Reissner, "A note on the problem of flexure of prismatical beams", *Int. J. Solids Struct.* **30**:4 (1993), 455–462.

[Schulz and Filippou 1998] M. Schulz and F. C. Filippou, "Generalized warping torsion formulation", *J. Eng. Mech.* (*ASCE*) **124**:3 (1998), 339–347.

[Sokolnikoff 1956]  I. S. Sokolnikoff, *Mathematical theory of elasticity*, McGraw-Hill, New York, 1956. Pages 91–248.

[Tapley and Poston 1990]  B. D. Tapley and T. R. Poston (editors), *Eshbach's handbook of engineering fundamentals*, 4th ed., Wiley-Interscience, New York, 1990. Pages 4–26.

[Timoshenko and Goodier 1984]  S. Timoshenko and J. N. Goodier, *Theory of elasticity*, 3rd ed., McGraw-Hill, New York, 1984. Pages 258–313.

[Williams and Johnson 1989]  J. L. Williams and W. J. H. Johnson, "Elastic constants of composites formed from PMMA bone cement and anisotropic bovine tibial cancellous bone", *J. Biomech.* **22**:6–7 (1989), 673–682.

[Young and Budynas 2002]  W. C. Young and R. G. Budynas, *Roark's formulas for stress and strain*, 7th ed., McGraw-Hill, New York, 2002. Pages 129 and 401.

LAMPROS C. KOURTIS: kourtis@stanford.edu
*Bone and Joint Center of Excellence, VA Palo Alto Health Care System, Palo Alto, CA 94304, United States*

and

*Biomechanical Engineering Division, 496 Lomita Mall, Room 226, Stanford University, Stanford, CA 94305, United States*

HANEESH KESARI: haneesh@stanford.edu
*Mechanics and Computation Division, Department of Mechanical Engineering, 496 Lomita Mall, Stanford University, Stanford, CA 94305, United States*

DENNIS R. CARTER: dcarter@stanford.edu
*Bone and Joint Center of Excellence, VA Palo Alto Health Care System, Palo Alto, CA 94304, United States*

and

*Biomechanical Engineering Division, 496 Lomita Mall, Room 226, Stanford University, Stanford, CA 94305, United States*

GARY S. BEAUPRÉ: beaupre@va51.stanford.edu
*Bone and Joint Center of Excellence, VA Palo Alto Health Care System, Palo Alto, CA 94304, United States*

and

*Biomechanical Engineering Division, 496 Lomita Mall, Room 226, Stanford University, Stanford, CA 94305, United States*